Bulletin of the Seismological Society of America, Vol. 101, No. 5, pp. 2542–2549, October 2011, doi: 10.1785/0120100176

Ⓔ

Short Note

Paleoseismic Trenches across the Sierra Nevada and Carson Range Fronts in Antelope Valley, California, and Reno, Nevada

by Alexandra C. Sarmiento, Steven G. Wesnousky, and Jayne M. Bormann*

Abstract Offset Quaternary deposits, measurements of fault scarps, and the excavation of two trenches along the eastern Sierra Nevada range front provide information on the rate and style of active faulting in Antelope Valley, California, and Reno, Nevada. Structural, stratigraphic, and pedogenic relations exposed in a trench in Antelope Valley (~38.6° N latitude) record two Holocene surface-rupturing earthquakes. Radiocarbon dates place the most recent and penultimate events at about 1350 calibrated years before present (cal B.P.) and older than about 6250 cal B.P., respectively. An approximate fault-slip rate of ~0.7 mm/yr is calculated by dividing the 3.6-m offset that occurred in the most recent event by the time between the two radiocarbon ages (~5000 years). A second trench excavated across the Carson Range frontal fault in Reno, Nevada (~39.4° N latitude) revealed a sharp, planar, low-angle failure surface dipping 33° E, lending to the possibility that the active normal fault is characterized by a dip much lower than expected from standard frictional considerations.

Online Material: High-resolution photomosaics of trench exposures.

Introduction

We present observations from two paleoseismic studies along the eastern Sierra Nevada range front and within the central and northern Walker Lane (Fig. 1). The Walker Lane is a zone of active normal and strike-slip faults that trends northwesterly along the eastern flank of the Sierra Nevada. Geodetic studies indicate that 15%–25% of the Pacific–North American right-lateral plate boundary transform motion is localized in the Walker Lane (DeMets and Dixon, 1999; Bennett *et al.*, 2003). The study focuses on the two north-striking normal faults that bound the eastern flank of the Sierra Nevada in Antelope Valley, California, and the Carson Range in Reno, Nevada (Fig. 1). Our observations provide information on the size and recurrence of earthquakes and the style of faulting in the two areas.

Observations

Antelope Valley

Antelope Valley is a north-northwest oriented basin located at approximately 38.6° N, 119.5° W. An approximately 23-km-long active fault trace bounds the western side of the valley and offsets young Quaternary deposits (Fig. 2). Displacement on the normal fault has produced an abrupt range front with triangular facets and has formed scarps in young alluvium at numerous fan heads (Fig. 2). North of the junction of U.S. Highway 395 and California State Route 89, the surface expression of the fault is disturbed by the highway and locally submerged by Topaz Lake. The abrupt and over steepened range front west of Holbrook Junction suggests that the fault system may discontinuously extend to the northwest another ~7 km, yielding a total length of 30 km or more.

We constructed scarp profiles at sites along the range front that have well-preserved scarps in young alluvium. The scarp heights range from 2.4 to 6.3 m (Fig. 2), and the profiles are cataloged by Sarmiento (2010). We excavated a trench perpendicular to the well-preserved scarp at site 4 (Fig. 2). Here the scarp strikes ~N20° E, and displacement on the fault has produced a scarp with ~5.6 m of vertical separation across young fan-head alluvium at the mouth of a large drainage along the range front.

The trench at site 4 exposed a fault that dips ~56° E, juxtaposing debris-flow deposits (Unit 5) against scarp-derived colluvium (Units 3 and 4) (Fig. 3 and Ⓔ Fig. S1, available in the electronic supplement to this paper). We

*Also at: Nevada Geodetic Laboratory, Nevada Bureau of Mines and Geology, University of Nevada, Reno, Mail Stop 178, Reno, NV 89557.

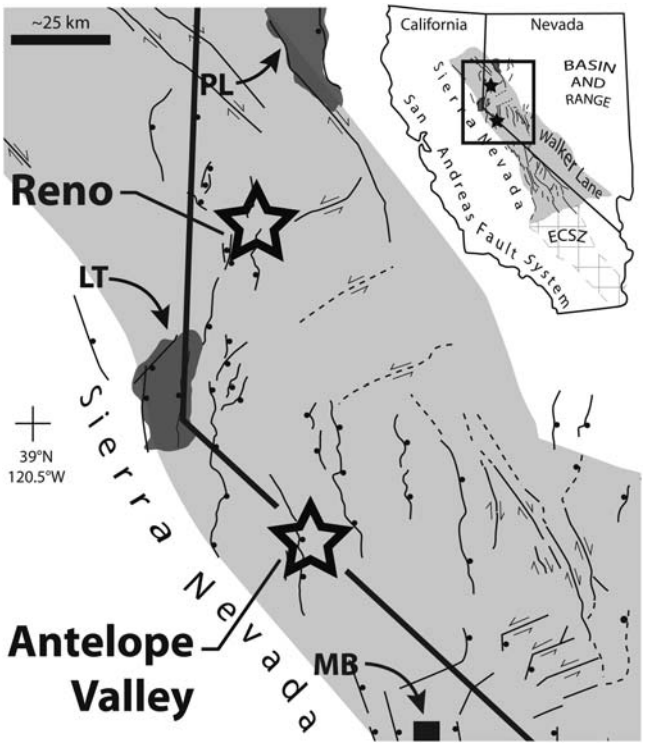

Figure 1. (Right) Regional map showing the generalized tectonic provinces in eastern California and western Nevada modified from Wallace (1984), Stewart (1988), Dokka and Travis (1990), dePolo *et al.* (1997), Bennett *et al.* (2003), Briggs and Wesnousky (2004), Wesnousky (2005), and Bacon and Pezzopane (2007). The Walker Lane (shaded grey area) and the Eastern California Shear Zone (ECSZ) (gridded-hatching) accommodate ~1 cm/yr of northwest-directed right-lateral shear (e.g., Thatcher *et al.*, 1999; Bennett *et al.*, 2003). The rectangle in the inset map shows the area of detail to the left. (Left) Detailed map showing selected faults (arrows show sense of strike-slip displacements, and balls are on the downthrown side of dip-slip faults). Large stars show study sites in Reno and Antelope Valley. PL, LT, and MB indicate Pyramid Lake, Lake Tahoe, and Mono Lake basin, respectively.

distinguished three subunits (5a, 5b, and 5c) in Unit 5 based on differing clast size and clast concentrations. In the footwall, west of the logged exposure, Unit 5c is overlain by a weak Bt soil horizon (cf. Birkeland, 1999) that is approximately 20 cm thick. No pedogenic carbonate has accumulated below the Bt horizon. A fissure (Unit 6) extends from the bottom of the exposure to within ~0.5 m of the ground surface.

We define four units in the hanging wall of the trench. Units 1 and 2 are at the base of the exposure in the hanging wall. Units 1a and 1b consist of east-dipping, moderately to well-sorted, thinly bedded sand and gravel stream alluvium deposits that are separated by Unit 2, a massive, poorly sorted, sub-rounded to angular debris flow deposit in a sandy matrix. Units 1 and 2 are overlain by Unit 3, a fining-upward and thinning-eastward wedge-shaped gravel deposit that abuts the fault. Near the fault, clasts in Unit 3 are aligned downslope, and the sand matrix has shear fabric that is parallel to the fault. Very weak, discontinuous blocky peds near the top of Unit 3, close to the fault, appear to be evidence of incipient soil development.

The youngest unit in the trench is Unit 4, a wedge-shaped deposit of pebbles and cobbles in a sandy matrix abutting the fault. Its basal contact with Unit 3 is characterized by a distinctly coarser matrix and larger clast size than that occurring in Unit 3. A small fissure along the fault is filled with Unit 4 sand. Unit 4 is exposed on the surface and rests on the scarp face.

We interpret Units 3 and 4 to be scarp-derived colluvium from surface ruptures related to the penultimate and most recent earthquakes, respectively. The juxtaposition of Unit 4 against the fault, its stratigraphic position on the scarp face, and the fault-aligned clasts within the fissure fill support the interpretation that Unit 4 is scarp-derived colluvium from the most recent earthquake. The very weak, discontinuous soil development in the top of Unit 3 indicates a surface that was somewhat stabilized prior to burial by Unit 4. We estimate the net displacements on the fault plane from the most recent and penultimate events to be 3.6 and 3.1 m, respectively, based on the thickness of the colluvial wedge deposits along the fault plane. Reconstruction of the exposed cross-section to account for the two displacements appears to result in juxtaposition of Units 1a and 5 across the fault. The mismatch of units across the fault would suggest that the fault was also active prior to the earthquakes that resulted in the formation of colluvial Units 3 and 4.

Radiocarbon dating of a bulk sample from the top of Unit 3 that we interpret to be the soil developed at the event horizon for the most recent earthquake yields an age of 1312–1414 calibrated years before present (cal B.P.) (see sample AV2-SGW-Bulk in Table 1 and Fig. 3). We collected a second bulk sample for radiocarbon analysis from a relatively dark zone of fine sand just above the coarser cobble and small boulder-bearing base of the penultimate colluvial wedge Unit 3. Radiocarbon dating of the sample yielded an age of 6196–6294 cal B.P. (see sample AV5-SGW-Bulk in Table 1 and Fig. 3). Presuming the coarser material at the base of the colluvium was deposited shortly after the scarp formed, we infer that deposition of the sample occurred relatively close in time to the surface rupture that resulted in deposition of the colluvium in Unit 3. The apparent mean residence time radiocarbon ages obtained from these bulk samples provide only a maximum bound on the age of the horizon from which they are sampled and are coupled with uncertainties of tens to hundreds of years (Machette *et al.*, 1992; Birkeland, 1999; Anderson *et al.*, 2002).

Withstanding the uncertainties, the radiocarbon ages and structural and stratigraphic relations observed in the trench suggest that the inter-event time between the most recent and penultimate surface displacements is ~5000 years. Dividing the estimated net offset of 3.6 m in the most recent event by 5000 years suggests an inter-event fault-slip rate on the order of 0.7 mm/yr. The estimate assumes that all of the slip in the most recent event accrued as elastic strain subsequent

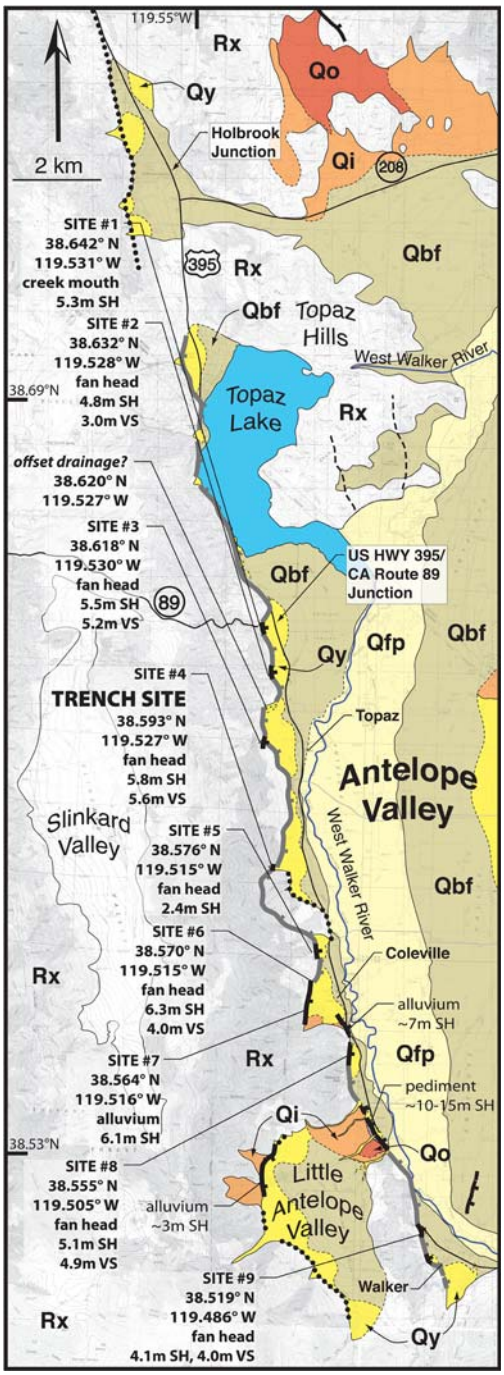

Figure 2. Quaternary geology and fault map of Antelope Valley showing measurements of fault scarps in young alluvium and site numbers. Details of scarp profiles are in Sarmiento (2010). All coordinates are World Geodetic System (WGS) 1984 datum. Units Qfp and Qbf are floodplain deposits and distal basin fill, respectively. Units Qy, Qi, and Qo are Quaternary alluvial deposits of latest Pleistocene–earliest Holocene, middle Pleistocene, and early Pleistocene ages, respectively. Unit Rx is undifferentiated bedrock. Scarp heights (SH) and vertical separations (VS) in bold and plain text are measured and estimated, respectively. Faults are shown by solid black lines where expressed in alluvium, and gray lines are along bedrock–alluvium contacts and are dotted where inferred. Lineaments on air photos are dashed black lines. The color version of this figure is available only in the electronic edition.

to the penultimate event and is a maximum in the sense that prior to the deposition of sample AV5-SGW-Bulk an unknown amount of time elapsed after the penultimate event.

The Antelope Valley fault trace extends northward at least ~23 km from its southern end to Topaz Lake or up to ~30 km if it continues yet further north to Holbrook Junction. Empirical regressions of rupture length to surface displacement and earthquake magnitude derived from historical data sets indicate that, on average, ruptures of this length result in earthquakes of magnitude 6.7–6.9 with average and maximum displacements of 0.5–0.9 m and 1.2–2.7 m, respectively (Wells and Coppersmith, 1994; Wesnousky, 2008). The offset in the most recent event is about 3.6 m at our trench site. The observation that the observed value of slip at the trench is relatively high compared to what is predicted from available empirical regressions is likely not significant. The published regression curves for normal faults in Wells and Coppersmith (1994) and Wesnousky (2008) are based on little data with large scatter. Thus, for example, one may note that the 23–30-km Antelope Valley fault length and the 3.6-m offset at the trench are similar to values reported for the 1959 M_s 7.5 Hebgen Lake earthquake which produced a 25-km-long surface rupture and average and maximum values of slip equal to 2.5 and 5.4 m, respectively (Doser, 1985; Wesnousky, 2008).

Carson Range

Active faulting along the east flank of the Carson Range in Reno has produced an abrupt range front, triangular facets, and a range-bounding scarp that cuts young alluvium (Fig. 4). We excavated a trench across a fault scarp ~900 m north of Thomas Creek (Figs. 4 and 5). The Qo surface of Figure 5 that extends eastward from the trench site is a pediment with a well-developed Bt and Bk soil horizon (cf. Birkeland, 1999) developed on the Hunter Creek Sandstone (Bonham and Rogers, 1983) and has been interpreted by Ramelli *et al.* (2007) to be middle Pleistocene in age. Numerous faults forming horst-and-graben structures are distributed across the Qo surface. A narrow zone of Holocene-active faults cutting the Qi surface have formed a graben between the Carson Range and Steamboat Hills. Radiocarbon dating of fissure-fill deposits has been interpreted to suggest that a number of these strands, including the frontal fault, experienced displacements ~900 radiocarbon years before present (^{14}C B.P.), perhaps in a single event (Fig. 5) (Bell *et al.*, 1984; Ramelli *et al.*, 2007).

The range-bounding scarp is continuously expressed in alluvial deposits from the trench site to the mouth of Thomas Creek, where progressive displacement is recorded by greater offsets of the Qy and Qo surfaces (Figs. 4 and 5). The trench is located at an embayment in the range front where the fault cuts outboard the range front and across a thin alluvial apron that overlies the Hunter Creek Sandstone. The scarp at the trench site has a height of ~6.3 m and vertical separation of ~1.5 m. The profile is cataloged in Sarmiento (2010). A log of the

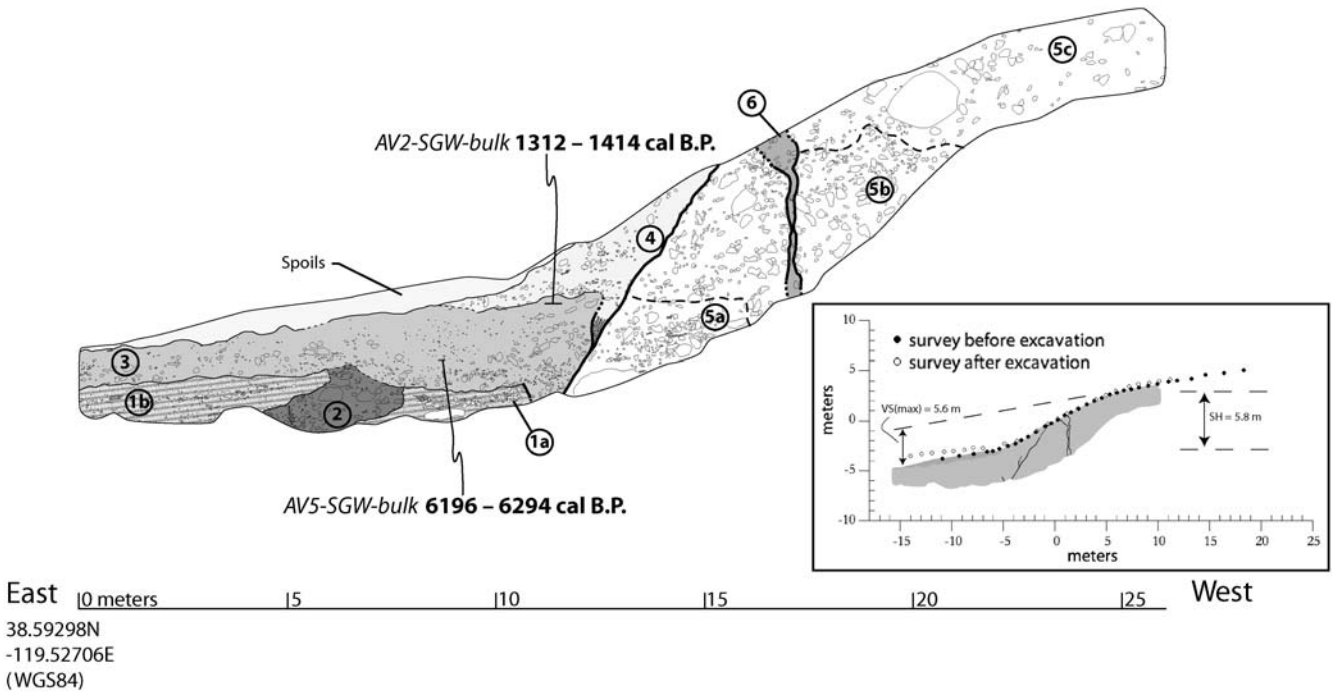

Figure 3. Map of the south wall of the Antelope Valley trench with no vertical exaggeration. The site location is indicated in Figure 2. Radiocarbon dating of bulk samples (Table 1) indicates that the most recent earthquake occurred about 1350 cal B.P., and the penultimate event occurred shortly before about 6250 cal B.P (see text for discussion). Ⓔ A photomosaic of the exposure (Fig. S1) is available as an electronic supplement to this paper. The inset box on the right is a scarp profile at the trench site. The area of the trench log is shown along profile as the shaded gray region. The mismatch between surveys before and after excavation is caused by surface disturbance during the excavation. Scarp height (SH) and vertical separation (VS) are shown on the profile.

trench is shown in Figure 6, and Ⓔ a photomosaic of the exposure is available as an electronic supplement to this paper in Figure S2.

The trench shows that the surface scarp is associated with a 33° eastward-dipping fault (Fig. 6). The footwall is composed of the Hunter Creek Sandstone (Unit 1), which dips eastward at a similarly low angle. The sandstone regionally consists of siltstone, fine sandstone, diatomaceous sandstone, and diatomite estimated to be 2.5–10.5 Ma in age (Bingler, 1975; Thompson and White, 1964; Kelly and Secord, 2009). The hanging wall (Unit 2) is a generally massive, poorly sorted, subangular gravel and cobble deposit in a sandy matrix. Texture and tonal changes allowed us to define several subunits. Unit 2c has generally smaller clasts than the surrounding parts of Unit 2 and a triangular shape that increases in width upward from the base of the exposure between meters 3 and 9 on the trench log. The western margin of Unit 2c is marked by an approximately 30-cm-wide zone of darker and looser matrix that is labeled Unit 2b in Figure 6. Unit 2d is similar in texture and color to Unit 2b

Table 1
Radiocarbon Analyses on Bulk Samples

Location	Sample Lab ID*	^{14}C Age† ±2σ	δ^{13}C‡ (‰)	Calendar age§ ±2σ (Years B.P.)	Calendar age§ ±2σ	Material
Unit 3, top	AV2-SGW-Bulk UGAMS# 04548	1495 ± 25	−22.2	1312–1414	536–638 A.D.	Soil
Unit 3, lower	AV5-SGW-Bulk UGAMS# 04549	5440 ± 30	−21.8	6196–6294	4345–4247 B.C.	Soil

*Samples processed at the University of Georgia Center for Applied Isotope Studies (CAIS) in Athens, Georgia. AV2-SGW-Bulk and AV5-SGW-Bulk are field sample numbers.

†Uses Libby half-life of 5568 years.

‡δ^{13}C values determined from the soil sample using a ^{14}C/^{13}C ratio.

§Dendrochronologically calibrated ages calculated with Web-based University of Washington calibration program (CALIB 5.0) (Stuvier and Reimer, 1986; Reimer *et al.*, 2004).

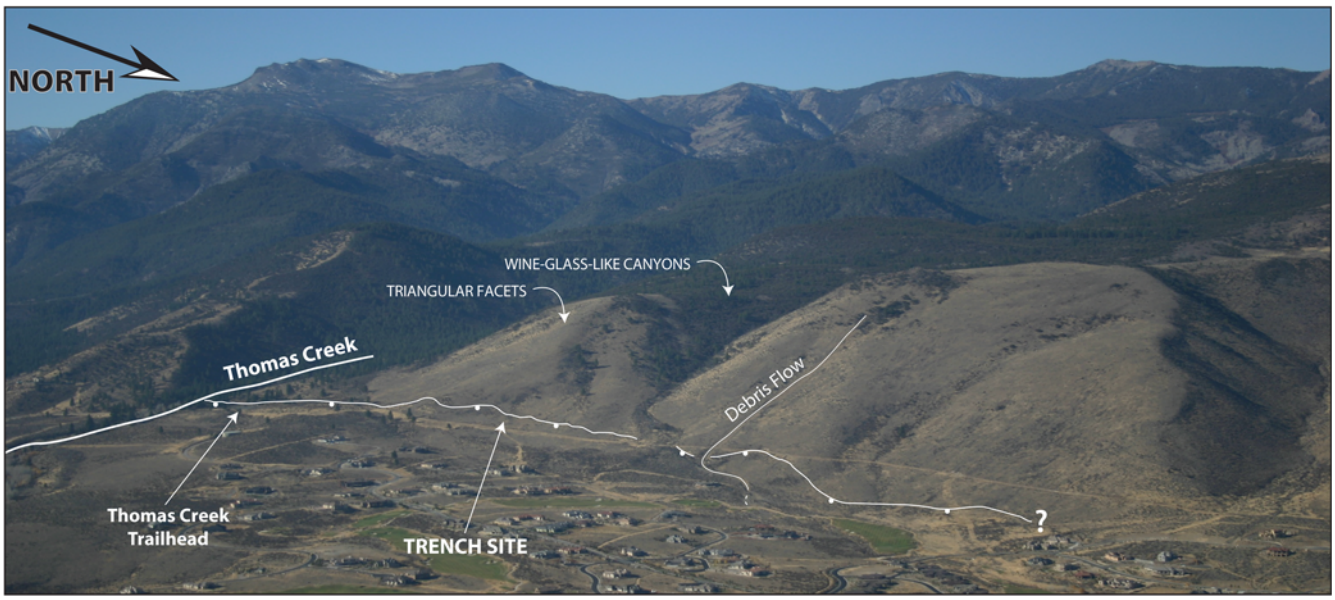

Figure 4. View to the southwest of the Carson Range in Reno, Nevada. Locations referred to in the text are annotated. The range-bounding fault is represented by the thin white line; balls are on the downthrown block. The abrupt range front has triangular facets and wine-glass canyons. Vertical relief exceeds 1525 m (5000 ft) from the valley floor in the foreground to the mountain peak in the upper left. The perspective of this photograph is indicated on the map in Figure 5. The color version of this figure is available only in the electronic edition.

and extends upward from the fault at meter 15 of the log. The entire exposure is capped by a soil that has well-developed Bt and Bk horizons. The Bt horizon is 0.25–0.5 m thick and has moderately strong, blocky peds commonly > 10 cm in size. The underlying Bk horizon is of similar thickness and has Stage II carbonate development. Bt horizons and Stage II Bk horizons generally have not formed on deposits that are younger than the last pluvial event in the western Great Basin (Adams and Wesnousky, 1999), and this degree of soil development probably requires on the order of 50,000 years or more to form (cf. Bell, 1995; Redwine, 2003; Koehler and Wesnousky, 2011; Kurth *et al.*, 2011).

We interpret Units 2b, 2c, and 2d to result from the opening, infilling, and shearing of Unit 2a subsequent to its deposition. The opening, infilling, and shearing occurred during sudden displacement along the low-dipping plane exposed in the trench. Because of the extensive shrink-swell properties of the overlying soil, it is not clear if the structures of Units 2b, 2c, and 2d extended to the surface and have since been obfuscated by soil-forming processes, or if the soil subsequently developed on them. These unclear relations, combined with the absence of dateable organic material, make it difficult to directly assess the timing of the most recent displacements or recurrence along the fault. Nonetheless, the well-developed soil does suggest that large offsets are not frequent.

A normal fault plane having such low dip is potentially significant to fault mechanics and seismic hazard analysis. The early work of Anderson (1951) shows that, from frictional considerations, normal faults should dip at angles around 60°, yet the fault in our trench dips at close to 30°. The association of the fault with a continuous scarp along the range front, progressive offsets of alluvial surfaces at the mouth of Thomas Creek, and an abrupt range front with triangular facets appears to favor a tectonic origin for the fault. It is not known to what depth the fault might extend at such a low angle; however, the dense distribution of faults outboard the range front producing the numerous horst-and-graben structures east of the trench may be evidence that it extends to at least a few kilometers in depth, as shattering of the thin veneer of hanging-wall deposits might be expected to occur with displacement on a shallow, low-angle normal fault. Consequently, the faults outboard the range front may sole into a low-angle normal fault and thus may not be independent seismic sources.

It is also currently unknown to what length the fault might extend at such a low angle along strike. An early report of a trench exposure along this same trace about 2 km south of our site at Whites Creek shows a near-vertical fault plane in alluvium near the surface with ~60 cm of fault displacement younger than 910 ± 70 ^{14}C B.P. (Bell *et al.*, 1984; Szecsody, 1983; Schilling and Szecsody, 1982) (Fig. 5). The steeper dip at Whites Creek may reflect a real change in fault dip or may simply be the typical steepening observed in normal fault planes as they enter less consolidated sediments near the surface. Whether or not the young 60-cm offset reached our trench is uncertain. The two sites may have not ruptured simultaneously, or the small offset in the thick and active soil on a fault of such low dip may readily be hidden.

Alternative interpretations of the low-angle fault are possible. One explanation might be that the scarp we trenched is the head scarp of a landslide that is being

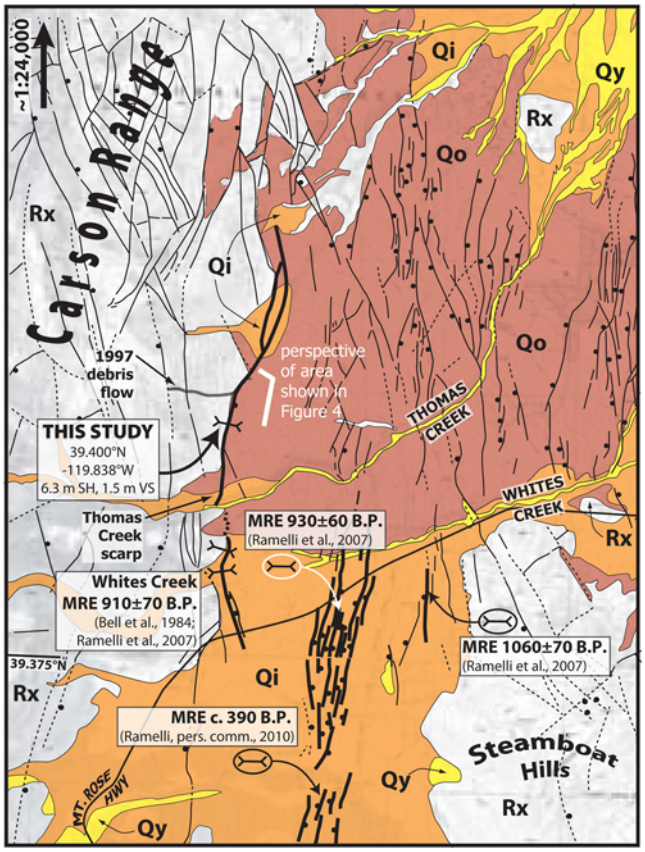

Figure 5. Quaternary geology map of the eastern flank of the Carson Range in Reno, Nevada, modified from Bonham and Rogers (1983), Szecsody (1983), Tabor and Ellen (1975), and Ramelli *et al.* (2007). Units Qy, Qi, and Qo are Quaternary alluvial deposits of latest Pleistocene–earliest Holocene, middle to late Pleistocene, and early to middle Pleistocene ages, respectively. Unit Rx is undifferentiated bedrock. The thick black lines are faults with Holocene displacement; thin black lines are faults with Pleistocene or older movement. Locations of previous paleoseismic studies and radiocarbon ages (^{14}C B.P.) of most recent earthquake (MRE) ruptures are given. The trench site for this study is identified (coordinates are WGS 1984 datum). The perspective of the range front photograph in Figure 4 is indicated. The color version of this figure is available only in the electronic edition.

accommodated by bedding plane slip within the Hunter Creek Sandstone. The absence of a landslide toe downslope of the scarp diminishes the viability of a landslide hypothesis (Sarmiento, 2010), as does the recognition that the fault a few hundred meters south along strike produces progressively greater offsets of alluvial terrace surfaces at the mouths of Thomas and Whites Creeks. In either case, the fault in this exposure is potentially significant in efforts to define seismic hazard in the region. For example, if indeed the active fault is of low angle, then predictions of strong ground motion would likely increase greatly because of the fault's proximity to the surface as compared to a fault of steeper dip. Additionally, the numerous horst-and-graben structures east of the trench may not in themselves be significant independent sources of strong ground motion because they probably sole into the low-angle fault at shallow depth.

Summary and Conclusions

Fault scarps that vertically offset young alluvial fan deposits along the Antelope Valley fault suggest that the most recent surface rupture was at least 23 km long. We exposed evidence of two surface-rupturing Holocene earthquakes in a trench across a 5.8-m-high scarp. Radiocarbon dating of bulk soil samples suggests that the most recent earthquake occurred about 1350 cal B.P., and the penultimate event occurred prior to about 6250 cal B.P. An approximate inter-event fault-slip rate of ~0.7 mm/yr may be calculated by dividing the 3.6-m offset that occurred in the most recent event by the time between the two radiocarbon ages (~5000 years). The slip-rate estimate is coupled with a significant yet unquantifiable uncertainty because it is averaged over a short time period and only one recurrence interval.

Active uplift of the Carson Range is expressed by distinct triangular facets, wine-glass canyons, and scarps in young alluvium along an abrupt range front. Our trench excavated in Reno along the range front near the northern limit of the clearly defined range-bounding fault reveals a low-angle normal fault that locally dips 33° near the surface. Structural, stratigraphic, and pedogenic relations in the trench are insufficient to elucidate an earthquake event history, although it appears that large offsets do not occur frequently. The depth and length along strike to which the low-angle dip of the fault extends remains unknown.

Finally, we note that the strike of these normal faults is approximately parallel to the long-term and ongoing right-lateral shear in the Walker Lane (e.g., Wesnousky, 2005) and, hence, the direction of slip observed on the faults in the trenches is not oriented in a manner to accommodate right-lateral shear in the Walker Lane but rather quite orthogonal. As well, long-term morphological indicators (i.e., abrupt range fronts, triangular facets) along the two fault systems indicate the major component of motion along the two faults studies is normal. Though some component of lateral slip might be hidden in the offsets preserved along the two faults (Sarmiento, 2010), it remains unclear exactly how these faults accommodate the northwest-directed right-lateral shear that is currently occurring in the Walker Lane.

Data and Resources

All data used in this paper were acquired in this study or came from published sources listed in the references.

Acknowledgments

We thank Alyce Brannigan of the United States Forest Service (USFS) Reno/Sparks office for assistance obtaining trenching permission in the Carson Range study and for her interest and enthusiasm. Thanks also go to Joe Garrato of the USFS Carson office, Michon Eban of the Reno/Sparks Indian Colony, Cheryl Seath and the folks at the Bureau of Land Management Bishop office, and Chris Wills of the California Geological Survey. We thank

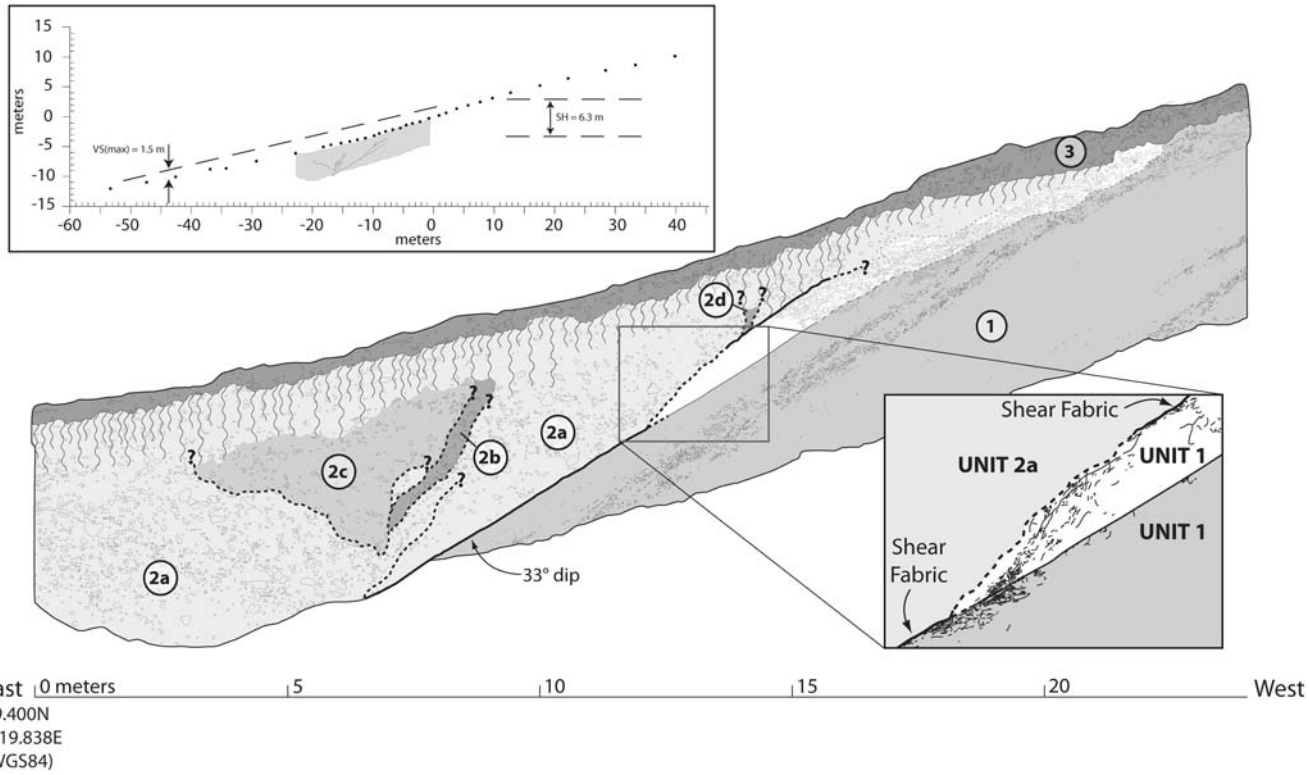

Figure 6. Map of the south wall of the Carson Range trench. No vertical exaggeration. The site location is shown in Figure 5. The sharp, planar, low-angle failure surface dips 33° E and is coincident with a bedding plane in the Hunter Creek Sandstone (Unit 1). Units 2b, 2c, and 2d are the result of opening, filling in, and shearing subsequent to deposition of Unit 2a. The fault loses definition in the well-developed Bt and Bk horizon in the hanging wall and may or may not extend into the soil. An Av horizon caps the exposure (Unit 3). See text for discussion. Ⓔ A photomosaic of the exposure (Fig. S2) is available as an electronic supplement to this paper. The inset on the left shows a scarp profile at the trench site. The area of the trench log is shown along profile as the shaded gray region. The scarp height (SH) and vertical separation (VS) are shown on profile.

Kelvin Berryman, Anthony Crone, and Alan Ramelli for particularly constructive reviews of the manuscript. A. C. Sarmiento wishes to thank Rich Koehler, Craig dePolo, Stephanie Watts, Tristan Ashcroft, Shane Smith, and Amber Ponder for valuable discussions and field assistance. This research was supported by National Science Foundation grants EAR-0635757 and EAR-0609556 and Center for Neotectonic Studies contribution 57.

References

Adams, K. D., and S. G. Wesnousky (1999). The Lake Lahontan highstand: Age, surficial characteristics, soil development, and regional shoreline correlation, *Geomorphology* **30,** 357–392, doi 10.1016/S0169-555X(99)00031-8.

Anderson, E. M. (1951). *The dynamics of faulting and dyke formation with applications to Britain*, Oliver & Boyd, Edinburgh, 206 pp.

Anderson, K., S. Wells, and R. Graham (2002). Pedogenesis of vesicular horizons, Cima volcanic field, Mojave Desert, California, *Soil Sci. Soc. Am. J.* **66,** 878–887.

Bacon, S. N., and S. K. Pezzopane (2007). A 25,000-year record of earthquakes on the Owens Valley fault near Lone Pine, California: Implications for recurrence intervals, slip rates, and segmentation models, *Bull. Geol. Soc. Am.* **119,** no. 7–8, 823–847, doi 10.1130/B25879.1.

Bell, J. W. (1995). Quaternary geologic map of the Mina quadrangle, Nevada, *Nevada Bur. Mines Geol. Field Stud. Map 10*, scale 1:24,000.

Bell, J. W., D. B. Slemmons, and R. A. Wallace (1984). Reno to Dixie Valley —Fairview Peak earthquake areas, in *Western geological Excursions*, J. Lintz Jr. (Editor), *1984 Annual Meetings of the Geological Society of America, Guidebook*, Reno, Nevada, 425–472.

Bennett, R. A., B. P. Wernicke, N. A. Niemi, A. M. Friederich, and J. L. Davis (2003). Contemporary strain rates in the northern Basin and Range province from GPS data, *Tectonics* **22,** no. 1008, 31, doi: 10.1029/2001TC001355.

Bingler, E. C. (1975). Guidebook to the Quaternary geology along the western flank of the Western Truckee Meadows, Washoe County, Nevada, in *Guidebook to Quaternary Geology, Truckee Meadows Geological Society of America 1975 Cordilleran Section Meeting*, Las Vegas, Nevada, Nevada Bureau of Mines and Geology Report No. 22.

Birkeland, P. W. (1999). *Soils and Geomorphology*, Third Edition, Oxford University Press, New York, 430 pp.

Bonham, H. F., and D. K. Rogers (1983). Geologic map of the Mt. Rose NE Quadrangle, Nevada, *Nevada Bur. Mines Geol. Map 4Bg*, scale 1:24,000.

Briggs, R. W., and S. G. Wesnousky (2004). Late Pleistocene faultfault sliphyphen;slip rate, earthquake recurrence, and recency of slip along the Pyramid Lake fault zone, northern Walker Lane, United States, *J. Geophys. Res.* **109,** no. B08402, 16, doi 10.1029/2003JB002717.

DeMets, C., and T. H. Dixon (1999). New kinematic models for Pacific—North America motion from 3 Ma to present: I. Evidence for steady motion and biases in the NUVEL-1A model, *Geophys. Res. Lett.* **26,**, no. 13, 1921–1924, doi 10.1029/1999GL900405.

dePolo, C. M., J. G. Anderson, D. M. dePolo, and J. G. Price (1997). Earthquake occurrence in the Reno-Carson City Urban Corridor, *Seismol. Res. Lett.* **68,** no. 3, 401–412.

Dokka, R. K., and C. J. Travis (1990). Role of the eastern California shear zone in accommodating Pacific—North America plate motion, *Geophys. Res. Lett.* **17,** no. 9, 1323–1326.

Doser, D. I. (1985). Source parameters and faulting processes of the 1959 Hebgen Lake, Montana, earthquake sequence, *J. Geophys. Res.* **90,** no. B6, 4537–4556.

Koehler, R. D., and S. G. Wesnousky (2011). Late Pleistocene regional extension rate derived from earthquake geology of late Quaternary faults across the Great Basin, Nevada, between 38.5° and 40° N latitude, *Bull. Geol. Soc. Am.* **123,** no. 3–4, 631–650.

Kelly, T. S., and R. Secord (2009). Biostratigraphy of the Hunter Creek Sandstone, Verdi Basin, Washoe County, Nevada, *Spec. Pap. Geol. Soc. Am.* **447,** 133–146.

Kurth, G., F. M. Phillips, M. C. Reheis, J. L. Redwine, and J. B. Paces (2011). Cosmogenic nuclide and uranium-series dating of old, high shorelines in the western Great Basin, USA, *Bull. Geol. Soc. Am.* **123,** no. 3–4, 744–768.

Machette, M. N., S. F. Personius, and A. R. Nelson (1992). Paleoseismology of the Wasatch fault zone: A summary of recent investigations, interpretations, and conclusions, in *Assessment of Regional Earthquake Hazards and Risk Along the Wasatch Front, Utah*, P. L. Gori and W. W. Hays (Editors), *U S Geol. Surv. Prof. Pap. 1500-A*, 71 pp.

Ramelli, A. R., C. M. dePolo, and J. W. Bell (2007). Paleoseismic studies of the Little Valley fault, *U S Geol. Surv. Final Tech. Report, no. 02HQGR0103*, 26 pp.

Redwine, J.L. (2003). The Quaternary pluvial history and paleoclimate implications of Newark Valley, east-central Nevada; derived from mapping and interpretation of surficial units and geomorphic features, *Master's Thesis*, Humboldt State University at Arcata, California, 358 pp.

Reimer, P. J., M. G. L. Baillie, E. Bard, A. Bayliss, J. W. Beck, C. Bertrand, P. G. Blackwell, C. E. Buck, G. Burr, K. B. Cutler, P. E. Damon, A. G. Hogg, K. A. Hughen, B. Kromer, F. G. McCormac, S. Manning, R. W. Reimer, S. Remmele, J. R. Southon, M. Stuvier, S. Talamo, F. W. Taylor, J. van der Plicht, and C. E. Weyhenmeyer (2004). IntCal04 terrestrial radiocarbon age calibration, 0–26 cal kyr BP, *Radiocarbon* **46,** no. 3, 1029–1058.

Sarmiento, A.C. (2010). Earthquake recurrence and modes of deformation in the central and northern Walker Lane: Observations from paleoseismic trenches across the Carson and Sierra Nevada range fronts, *Master's Thesis*, University of Nevada at Reno, 142 pp.

Schilling, J., and G. C. Szecsody (1982). Earthquake hazard maps, Mt. Rose NE and Reno NW $7\frac{1}{2}$ minute quadrangles: Nevada Bureau of Mines and Geology final technical report, *U S Geol. Surv. National Earthquake Hazard Reduction Program, Contract 14-08-0001-19823*, 63 pp.

Stewart, J. H. (1988). Tectonics of the Walker Lane Belt, western Great Basin—Mesozoic and Cenozoic deformation in a zone of shear, in *Metamorphism and crustal evolution of the western United States*, W. G. Ernst (Editor), Prentice Hall, New Jersey, 683–713.

Stuiver, M., and P. J. Reimer (1986). A computer program for radiocarbon age calibration, *Radiocarbon* **28,** 1022–1030.

Szecsody, G. C. (1983). Earthquake hazards map of Mt. Rose NE Quadrangle, Nevada, *Nevada Bur. Mines Geol. Map 4Bi*, scale 1:24,000.

Tabor, R. W., and S. Ellen (1975). Geologic map of the Washoe City quadrangle, *Nevada Bur. Mines Geol. Environmental Series, Map 5Ag*, scale 1:24,000.

Thatcher, W., G. R. Foulger, B. R. Julian, J. L. Svarc, E. Quilty, and G. W. Bawden (1999). Present-day deformation across the Basin and Range province, western United States, *Science* **283,** 1714–1717, doi 10.1126/science.283.5408.1714.

Thompson, G. A., and D. E. White (1964). Regional geology of the Steamboat Springs area, Washoe Valley, Nevada, *U. S. Geol. Surv. Prof. Pap. 458A*, 52 pp.

Wallace, R. E. (1984). Patterns and timing of late Quaternary faulting in the Great Basin province and relation to some regional tectonic features, *J. Geophys. Res.* **89,** 5763–5769.

Wells, D. L., and K. J. Coppersmith (1994). New empirical relationships among magnitude, rupture length, rupture width, rapture area, and surface displacement, *Bull. Seismol. Soc. Am.* **84,** 974–1002.

Wesnousky, S. G. (2005). Active faulting in the Walker Lane, *Tectonics* **24,** 35, doi 10.1029/2004TC001645.

Wesnousky, S. G. (2008). Displacement and geometrical characteristics of earthquake surface ruptures: Issues and implications for seismic-hazard analysis and the process of earthquake rupture, *Bull. Seismol. Soc. Am.* **98,** no. 4, 1609–1632, doi 10.1785/0120070111.

Center for Neotectonic Studies
University of Nevada, Reno
Mail Stop 169, Reno, NV 89557
sarmiento.alexandrac@gmail.com

Manuscript received 22 June 2010